

SYNTHESIS AND CHARACTERIZATION OF Al-Zn-Mg ALLOY / ZIRCON SAND REINFORCED COMPOSITES

Aluminium based metal matrix composite (Al-MMC's) are much popular in the field like automobile and aerospace industries, because of its ease of fabrication process and excellent mechanical properties. In this study, Al-Zn-Mg alloy composite reinforced with 3, 6 and 9 v % of zircon sand was synthesised by stir casting technique. The microstructure of the composites revealed uniform distribution of reinforced particles. Hardness, tensile strength and wear resistance of Al-Zn-Mg alloy/zircon sand composite were found to increase with increase in v % percentage of zircon sand. Scanning Electron Microscope analysis of wear tested sample surface of composites revealed no evidence of plastic deformation of matrix phase. Particle pulls out and abrasive wear was the common feature observed from all the composites.

Keywords: Al-Zn-Mg alloy, Microstructure, Hardness, Tensile strength, Wear.

1. Introduction

Aluminium alloys are widely used in aerospace and automobile industries due to their low density and good mechanical properties, better corrosion resistance and wear, low thermal coefficient of expansion as compared to conventional metals and alloys. The excellent mechanical properties of these materials and relatively low production cost make them as a attractive candidate of research [1,2]. Particulate reinforced composites have been reported to have a better plastic forming capability than whisker & fiber reinforced composites. Also they exhibit excellent heat and wear resistances due to the superior hardness and heat resistance characteristics of the particle distributed in the matrix [1]. There are several fabrication techniques available for manufacturing of Aluminium Metal Matrix Composites (Al-MMCs). These techniques include stir casting [3-5], squeeze casting [6], powder metallurgy [7,8], liquid metal infiltration [9], spray deposition [10] and mechanical alloying [11]. Stir casting route is practiced commercially due to its simplicity, flexibility and applicability to large quantity production [2,3,5].

Numerous research work have been reported on Aluminium reinforced with various particulates such as TiC [12], SiC [13], zircon sand [14], Al₂O₃ [15], B₄C [16] and Si₃N₄ [17]. Only very limited amount of work have been reported on zircon sand reinforced composites. Zircon sand possesses high hardness, excellent thermal stability and high modulus of elasticity which makes it a suitable reinforcement.

Ramakoteswara Rao [12] investigated the mechanical and tribological properties of AA7075-TiC metal matrix composites

under heat treated (T6) and cast conditions. They reported that the mechanical (hardness, tensile strength and percentage of elongation) properties of TiC reinforced composite specimens were better than AA7075 matrix material in both conditions. Kumar et al. [13] examinations have proved that addition of SiC particles to AA7075 alloy can significantly improve the wear resistance of matrix alloy. Satish et al. [14] found that addition of zircon and alumina to Al-Si-Mg alloy may lead to tremendous improvement in the hardness of the Al-Si-Mg alloy.

Hence in this work an attempt has been made to study the effect of zircon sand on microstructure and mechanical properties of Al-Zn-Mg alloy composites.

2. Experimental details**2.1. Materials**

In the present investigation, Al-Zn-Mg alloy was used as the matrix material and Zircon used as reinforcement. Composition of matrix alloy and zircon sand is shown in Table 1 and Table 2 respectively.

TABLE 1

Composition of Al-Zn-Mg alloy

Al-Zn-Mg alloy	Si	Cu	Mn	Mg	Zn	Cr	Ti	Al
Composition (wt %)	0.2	0.2	0.5	1.7	3.2	0.3	0.20	93.7

* PSG COLLEGE OF TECHNOLOGY, DEPARTMENT OF METALLURGICAL ENGINEERING, COIMBATORE-641004, TAMILNADU, INDIA.

** PSG COLLEGE OF TECHNOLOGY, DEPARTMENT OF PHYSICS, COIMBATORE-641 004, TAMILNADU, INDIA.

Corresponding author: satishmetly@gmail.com

TABLE 2

Composition of zircon sand

Zircon Sand	ZrO ₂	SiO ₂	TiO ₂	Fe ₂ O ₃	Volatiles
Composition (wt %)	65.80%	32.50%	0.20%	0.15%	1.35

2.2. Preparation of composites by stir casting method

Al-Zn-Mg alloy was charged into a graphite crucible and heated to 800°C till the entire metal in the crucible was melted. Zircon particles of size ranging from 74-88 μm were preheated to a temperature of 450°C for 2 h before incorporating into the melt to remove moisture. A stirrer made up of stainless steel was lowered into the melt slowly in to the molten metal to stir at a speed of 600 rpm. The melt temperature was reduced to 700°C and the preheated zircon particles were added into the molten metal at a constant rate during stirring. Stirring was continued for another 10 min even after completing the addition of particle to ensure uniform distribution of particles throughout the matrix. Hexachloroethane tablets were added to the melt to reduce porosity, and then the melt was poured into steel mould. Photograph of matrix alloy and zircon reinforced composites is shown in Fig. 1.

2.3. Density measurement

Density measurement for both the unreinforced alloy and the composite was carried out by Archimede's principle. The theoretical density for single reinforced composite sample can be estimated from the rule of mixtures.

$$\rho_t = \rho_m v_m + \rho_r v_r \quad (1)$$

where ρ_t is the theoretical density; ρ_m and ρ_r are the densities of the matrix and reinforcement respectively (g/cc); v_m and v_r are the volume fractions of matrix and reinforcement respectively.

2.4. Microstructural analysis

Microstructural analysis of the alloy and the composites was studied by using optical microscopy (Eclipse MA-100, Nikon) (Carl Zeiss). Samples were polished as per standard metallographic practice, etched with Keller's reagent and examined under optical microscope. Worn surface of wear tested composite samples were examined with SEM (JSM-5800). The SEM image was taken in secondary electron mode.

2.5. X-ray diffraction analysis

XRD analysis was carried out from 10° to 80° using SHIMADZU LabX-6000 model X-Ray Diffractometer to obtain the diffraction pattern of the synthesized samples with Copper-K α radiation ($\lambda = 1.5409 \text{ \AA}$). A scan speed of 2°/min with step scan of 0.02° was used to scan the sample.

2.6. Hardness test

Hardness of Al-Zn-Mg alloy as well as the composites was measured using a Brinell hardness tester using 10 mm steel ball indenter with a load of 500 kg as per ASTM E10 standard. An average of 5 readings at different places on each sample was taken as the hardness value.



Fig. 1. Photograph of matrix alloy (a) and zircon reinforced composites (b) 3 v % (c) 6 v % and (d) 9 v %

2.7. Tensile test

Samples of alloy and its composites were subjected to tensile tests using Hounsfield Tensometer. The samples were machined as per ASTM E8 standard, with a length of 36 mm, gauge length of 30 mm and dia 6 mm. The cross head speed was maintained at 2 mm/min.

2.8. Wear test

Dry sliding wear behaviour of the alloy and the composites were carried out at room temperature using a pin-on-disc wear and friction monitor (Model TR-20, Ducom, Bangalore). Cylindrical samples of length 30 mm and diameter 10 mm were tested against a hardened EN32 steel disc having a hardness of 65 HRC. This procedure was repeated three times and the wear rate was calculated by taking the average of the wear test results. Wear rate for the pin was calculated using the Eq. (2) as per ASTM standard G99.

$$W(\text{mm}^3 \text{m}^{-1}) = \frac{M(\text{g}) / D(\text{g}/\text{mm}^{-3})}{\text{sliding distance (m)}} \quad (2)$$

where M = mass loss during abrasive wear; D = density of the respective composite

3. Results and discussion

3.1. Density measurement

Fig. 2 shows the variation in measured density of the base alloy ($2.76 \text{ g}/\text{cm}^3$) and the zircon ($4.68 \text{ g}/\text{cm}^3$) reinforcement.

The reason for increase in density on increasing the v % of reinforcement can be attributed to the higher density of zircon sand. The theoretical densities were calculated from the rule

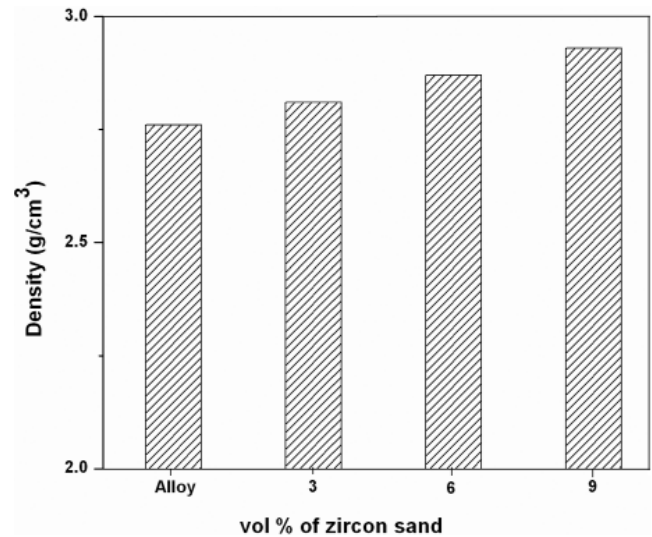


Fig. 2. Variation in density of composites with respect to different v % of zircon

of mixtures (Equation 1). As the porosity in all the composites are very less, the measured and calculated densities of all the composites are found to be nearly same.

3.2. XRD analysis

X-ray diffraction pattern for the composites is shown in Fig. 3. Pattern revealed the presence of Al, MgZn_2 [18-21] and ZrSiO_4 .

3.3. Microstructural analysis

Optical micrographs of the as-cast Al-Zn-Mg alloy Fig. 4a, Fig. 4b 3 v % Fig. 4c 6 v % and Fig. 4d 9 v % Zircon reinforced composites.

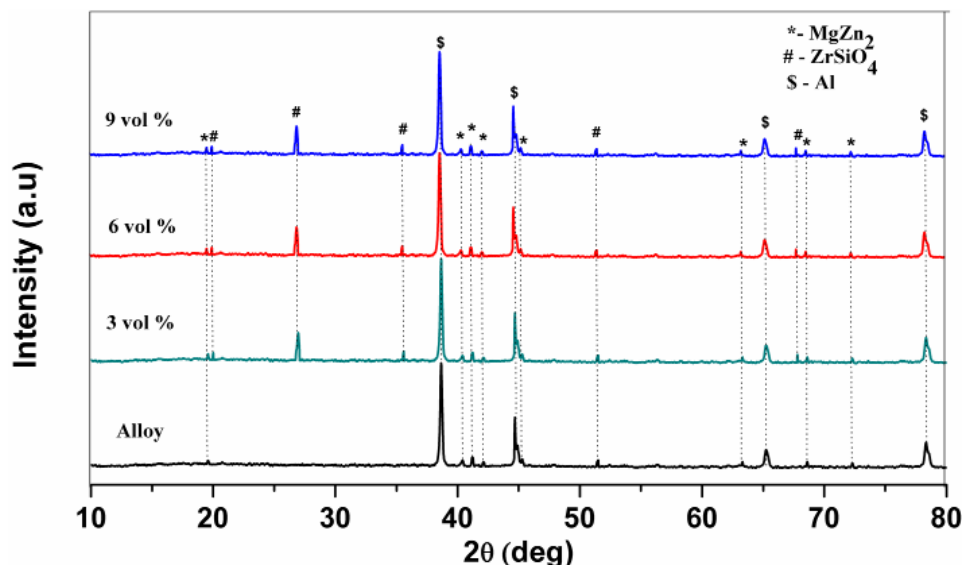


Fig. 3. XRD pattern Al-Zn-Mg alloy /zircon composites

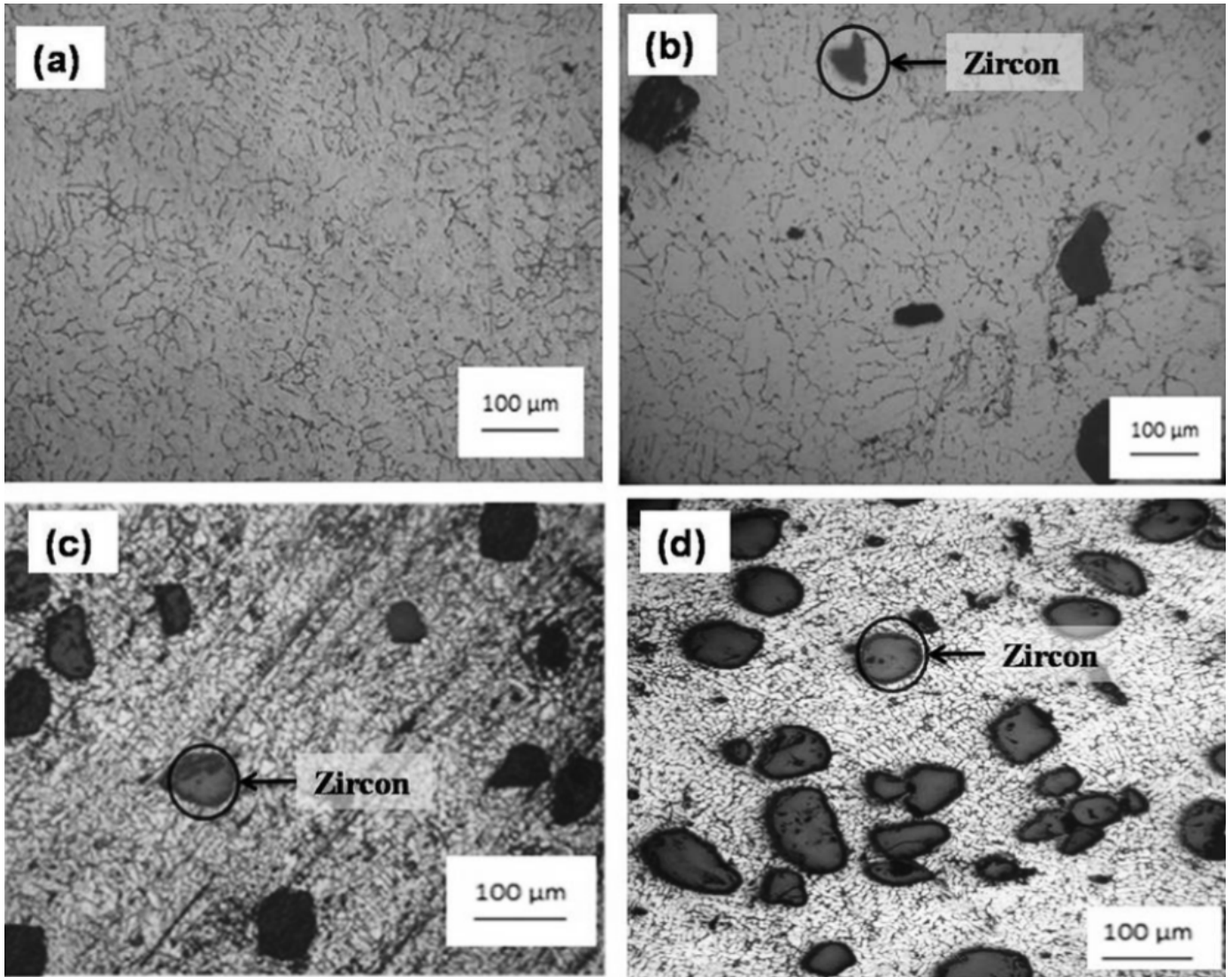


Fig. 4. Optical micrographs of (a) Al-Zn-Mg alloy and its composites (b) 3 v % (c) 6 v % and (d) 9 v %

Optical micrographs of zircon reinforced composite shows uniform distribution of zircon in the matrix. No void or discontinuities were observed from the microstructure. However, little amount of clustering was observed in the micrograph of 9 v % zircon sand reinforced composites. The refinement in matrix is due to the heterogeneous nucleation caused by the addition of addition of reinforcement particles into the matrix alloy [14,22-25]. As the v % of zircon increased, the size of the matrix became finer due to more heterogeneous nucleation sites.

3.4. Hardness test

Hardness values of age hardened alloy and composites are shown in Figure 5. From the graph, it is clear that the composites exhibit higher hardness than unreinforced alloy. This can be attributed due to the large difference in thermal expansion coefficient between the matrix and the reinforcement. This difference can lead to the generation of higher dislocation density in the matrix of the composite [14,26,27].

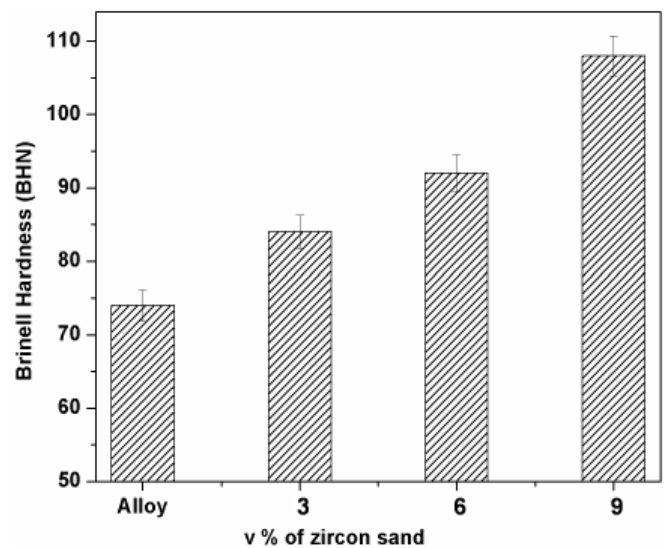


Fig. 5. Variation in hardness of the composites with respect to different v % of zircon

This increased dislocation density of Al-Zn-Mg alloy matrix leads to an increase in hardness of the composite compared to that of unreinforced alloy. In addition, presence of reinforcement particles tends to refine the matrix grain size which in turn improves the hardness of the composite [27]. Composite reinforced with 9 v % of zircon sand exhibits higher hardness. This is due to a combination of higher proportion of harder zircon particles along with good interfacial bonding rendered by both the reinforced particles.

3.5. Tensile test

Ultimate tensile strength of Al-Zn-Mg alloy and Al-Zn-Mg alloy /zircon composites are shown in Figure 6. The enhancement in ultimate tensile strength with increase in v % of reinforcement is partly due to the effective transfer of applied stress to the

zircon by matrix, grain refinement and particle strengthening of composites. It is expected that due to thermal mismatch stress, there is a possibility of increased dislocation density within the matrix during cooling from solidification temperature which restrict the deformation, thereby increasing the ultimate tensile strength. This is suggested as Orowan mechanism in which the dislocations bypass impenetrable obstacles to leave a dislocation loop around a particle. Thus interaction of dislocations with reinforcement can significantly improve the tensile strength [28]. Similar results were observed by Murali et al [29] and Onoro [30] in aluminum matrix reinforced with particles TiO_2 and TiB_2 particles respectively.

Figure 6b shows the % elongation of the alloy and the composites. The graph clearly shows that % elongation decreases with increase in v % of reinforcement particles. Similar results were observed by Ramakoteswara Rao et al. [12] in their study on AA7075-TiC metal matrix composites.

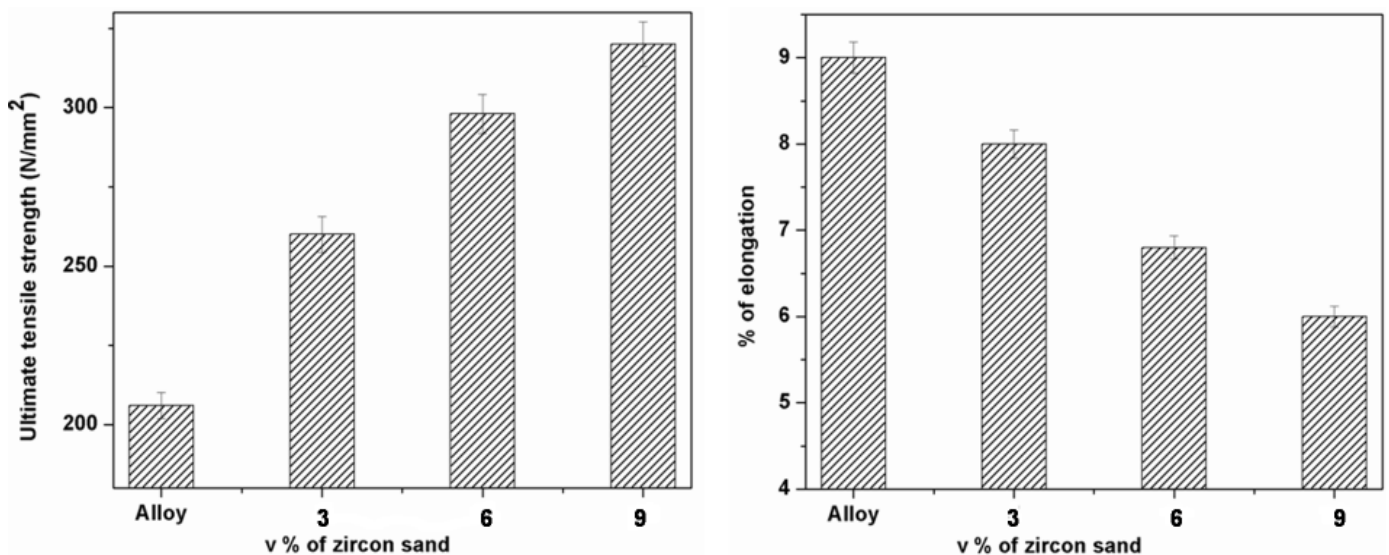


Fig. 6. (a) Ultimate tensile strength and (b) % elongation of Al-Zn-Mg alloy and Al-Zn-Mg alloy / zircon composites with different v % of reinforcement

3.6. Wear test

Effect of zircon on wear behavior of Al-Zn-Mg alloy and the composites at 15 N load shown in figure 7. From the wear test, wear rate of the composite was found to decrease with increase in v % of zircon particles. It was observed that the 9 v % of zircon reinforced composite exhibited better wear resistance compared to all other composites and base alloy.

All the composites were found to exhibit better wear resistance compared to that of the base alloy. Al-Zn-Mg alloy shows higher wear rate up to a sliding distance of about 1200 m and a gradual decrease thereafter. This is due to the strain hardening of the alloy on increasing the sliding distance [31].

During the first stage, all composites exhibit an increase in wear rate up to a sliding distance of about 1200 m. In the second stage, after 1200 m, the wear rate exhibits more or less a steady change. The variation in wear rate with sliding distance is due to

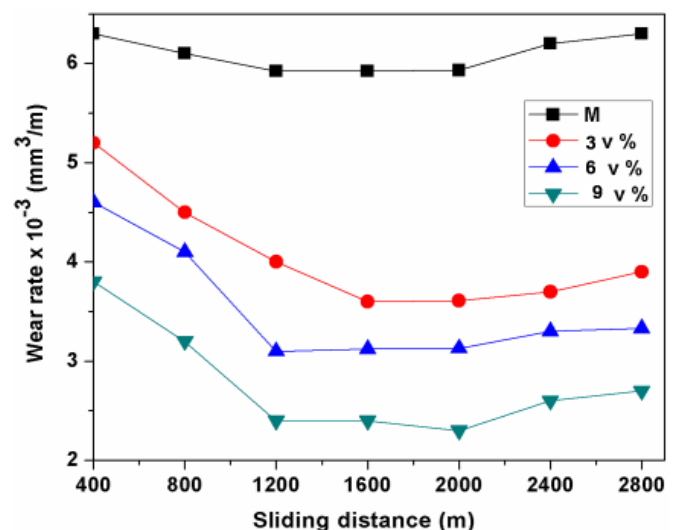


Fig. 7. Wear rate of Al-Zn-Mg alloy / different v % of zircon sand composites with varying sliding distance

the change in run in wear condition to steady state. The steady condition is achieved due to the material acquiring constant temperature between the sample surface and the steel disk surface. This is due to the fluctuations in wear rate during the initial stage of sliding. Similar results have been reported by Panwar et al. [32] for Al-Si alloy composite reinforced with different ratios of coarse and fine size zircon sand particles.

Figure 8a shows the worn surface of Al-Zn-Mg alloy, and the material loss is found to be very high along the sliding direction. Figure 6b, Figure 6c and Figure 6d shows respectively the worn surface of composite reinforced with 3 v %, 6 v % and 9 v %. Composites reinforced with 3 v %, 6 v % the micrographs reveal the formation of deeper abrasive grooves along the sliding direction leading to more material loss. Figure 6d shows the worn surface of the composite reinforced with 9 v % zircon and the SEM image reveals smooth surface with formation of shallow abrasive grooves along sliding direction indicating less material loss. However, Clustering of reinforcement particles

leads to pull out of particles from the matrix may get trapped between the pin and the disc further increasing the material loss by ploughing action.

4. Conclusions

Al-Zn-Mg alloy / zircon sand reinforced composites were successfully synthesized by stir casting technique. All the composites prepared were found to exhibit a higher density than the matrix alloy that can be attributed to the higher density of zircon. Microstructural examination revealed the uniform distribution of zircon particles in the matrix, with very limited segregation in few composites. Hardness and tensile strength for zircon sand reinforced composite are better than that of the base alloy. However, the % of elongation for the composites decreases with increase in v % of zircon sand. Composites exhibits better wear resistance compared to Al-Zn-Mg alloy. This can be attributed

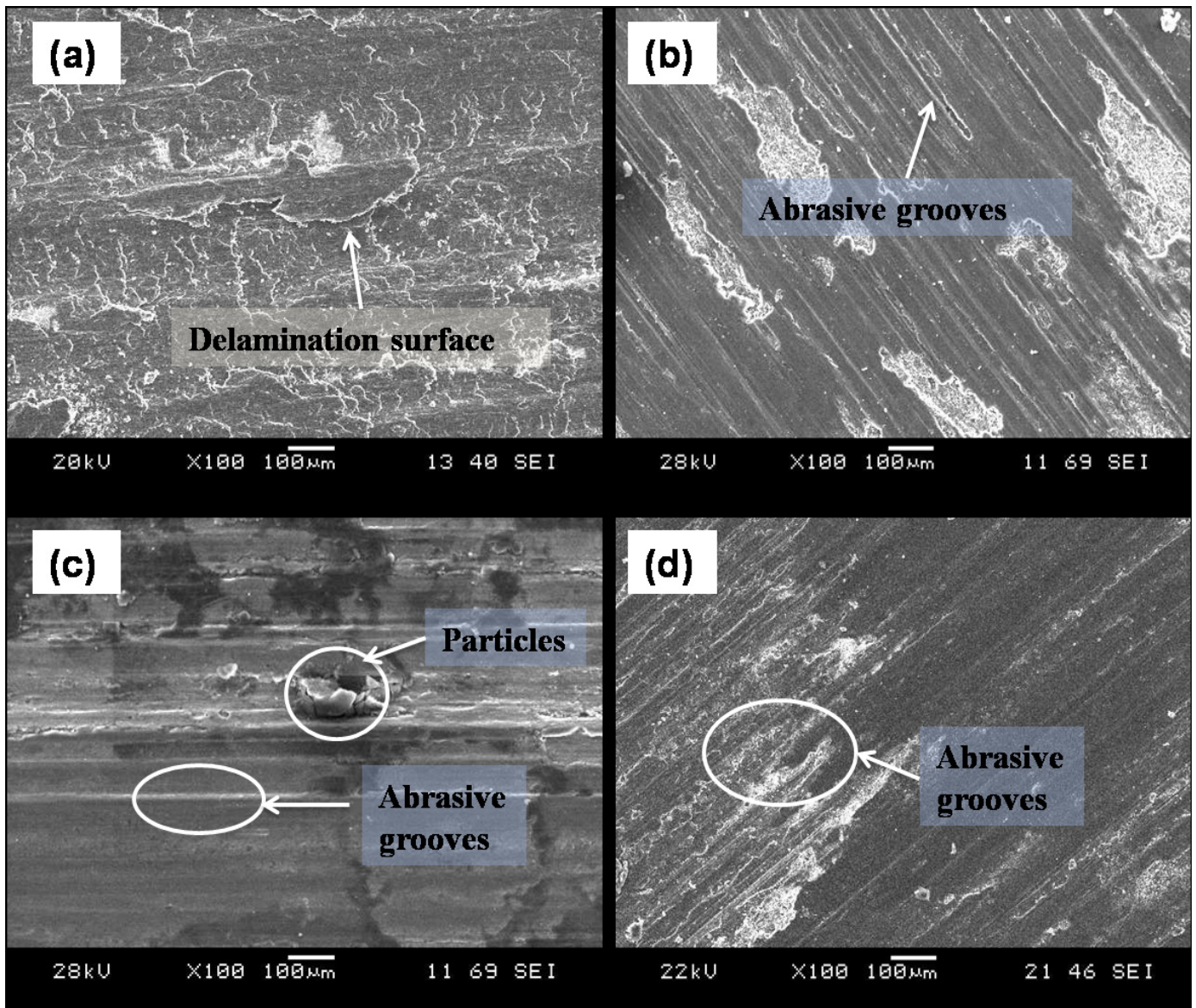


Fig. 8. Scanning electron micrograph of worn surface of (a) Al-Zn-Mg alloy, (b) 3 v % (c) 6 v % and (d) 9 v %

to the high hardness of zircon sand particles. SEM analysis of worn surface of hybrid composites shows no evidence of plastic deformation of matrix phase. Abrasive wear mechanism is the common feature observed from all the composites.

REFERENCES

- [1] A. Kumar, M. Kumar, R. Goyal, *IJIRST – International J. for Innovative Res. in Science & Technol.* **2**, 436-439 (2016).
- [2] T. Satish Kumar, R. Subramanian, S. Shalini, *J. Mater. Res. Technol.* **4**, 333-347 (2015).
- [3] T. Satish Kumar, R. Subramanian, S. Shalini, P.C. Angelo, *J. Scientific and Ind. Res.* **75**, 89- 94 (2016).
- [4] A. Banerji, M.K. Surappa, P.K. Rohatgi, *Metall. Trans. B.* **14B**, 273- 283 (1983).
- [5] S. Das, V. Udhayabanu, S. Das, K. Das, *J. Mater. Sci.* **41**, 4668-4677 (2006).
- [6] E.G. Okafor, V.S. Aigbodion, *Tribol. Ind.* **32**, 31-37 (2010).
- [7] J.U. Ejiofor, B.A. Okorie, R.G. Reddy, *J. Mater. Eng. Perform.* **6**, 326-334 (1997).
- [8] H. Abdizadeh, M. Ashuri, P.T. Moghadam, A. Nouribahadory, H.R. Baharvandi, *Mater. Des.* **32**, 4417-4423 (1997).
- [9] Y. Chen, D.D.L. Chung, *J. Mater. Sci.* **29**, 6069- 6075 (1994).
- [10] K.P. Kaur, O.P. Pandey, *J. Alloys Compd.* **503**, 410-414 (2010).
- [11] T. Weibgarber, B.E. Kieback, *J. Metastab. Nanocryst. Mater.* **8**, 275-283 (2000).
- [12] V. Ramakoteswara Rao, N. Ramanaiah, M.M. Mohiuddin Sarcar, *J. Mater. Res. Technol.* **5**, 377- 383 (2016).
- [13] S. Kumar, V. Balasubramanian, *Wear* **264**, 1026-1034 (2008).
- [14] T. Satish Kumar, R. Subramanian, S. Shalini, P.C. Angelo, *Forschung im Ingenieurwes.* **79**, 123-130 (2015).
- [15] J.M. Gomez de Salazar, M.I. Barrena, *Scripta Mater.* **44**, 2489-2495 (2001).
- [16] T.G. Nieh, R.F. Karlak, *Scr. Mater.* **18**, 25-28 (1984).
- [17] J.M. Praveen, K.L. Vishnu Kumar, *Procedia Eng.* **97**, 642-647 (2014).
- [18] Yan Liu, Daming Jiang, Wenlong Xie, Jie Hu, Boran Ma, *Mater. Charact.* **93**, 173-183 (2014).
- [19] S. Saikawa, G. Aoshima, S. Ikeno, K. Morita, N. Sunayama, K. Komai, *Arch. of Metall. and Mater.* **60**, 871-874 (2015).
- [20] S.Y. Park, W.J. Kim, *J. Mater. Sci. Technol.* **32**, 660-670 (2016).
- [21] Xinwei Li, Qizhou Cai, Bingyi Zhao, Yating Xiao, Bing Li, *J. Alloys Compd.* **675**, 201-210 (2016).
- [22] V.S. Aigbodion, J. King. *Saud. University-Eng. Sci.* **26**, 144-151 (2014).
- [23] A.N. Abdel-Azim, Y. Shash, S.F. Mostafa, A. Younan, *J. Mater. Process. Technol.* **55**, 199-205 (1995).
- [24] M.K. Surappa, *J. Mater. Process. Technol.* **63**, 325-333 (1997).
- [25] A. Banerji, M.K. Surappa, P.K. Rohatgi, *Metall. Mater. Trans. B.* **14B**, 273-283 (1983).
- [26] D. Dunand, A. Mortensen, *A. Mater. Sci. Eng. A.* **135**, 179-184 (1991).
- [27] S. Kumar, R.S. Panwar, O.P. Pandey, *Ceram. Int.* **39**, 6333- 6342 (2013).
- [28] B.K.C. Ganesh, W. Sha, N. Ramanaiah, A. Krishnaiah, *Mater. Des.* **56**, 480- 486 (2014).
- [29] M. Murali, M. Sambathkumar, M.S. Senthil Saravanan, *Univ. J. Mater. Sci.* **2**, 49-53 (2014).
- [30] J. On˜oro, *Ingeniería y Ciencia de los Materiales, ETSI, Industriales, Universidad Politécnica de Madrid, c/José Gutiérrez Abascal, 2, 28006 Madrid, Spain; 2011.*
- [31] S. Das, S. Das, K. Das, *Compos. Sci. Technol.* **67**, 746-751 (2007).
- [32] R.S. Panwar, S. Kumar, R. Pandey, O.P. Pandey, *Tribol. Lett.* (2014) DOI: 10.1007/s11249-014-0335-y.